IOPscience iopscience.iop.org

Home Search Collections Journals About Contact us My IOPscience

Vibrational density of states of rare-gas crystals doped with impurities

This content has been downloaded from IOPscience. Please scroll down to see the full text.

1983 J. Phys. C: Solid State Phys. 16 3435

(http://iopscience.iop.org/0022-3719/16/18/013)

View the table of contents for this issue, or go to the journal homepage for more

Download details:

IP Address: 200.80.22.166
This content was downloaded on 27/10/2016 at 18:35

Please note that terms and conditions apply.

You may also be interested in:

Density of states of disordered systems by the continued-fraction method. III
N V Cohan and M Weissmann

Density of states of disordered systems by the continued-fraction method. II
M Weissmann and N V Cohan

On the density of states of disordered alloys and their moments
N V Cohan, C A Efeyan and M Weissmann

Optical properties of crystals with impurities
M J Pinto and B Koiller

The effect of nonorthogonality in the density of states of some metallic disordered systems
M Weissmann and N V Cohan

Analysis of the density of states of binary alloys: I. Comparison with the CPA
P Lambin and J P Gaspard

Electronic structure of bulk and surface disordered alloys
M C Desjonqueres and F Cyrot-Lackmann

J. Phys. C: Solid State Phys., 16 (1983) 3435–3447. Printed in Great Britain

Vibrational density of states of rare-gas crystals doped with impurities

A Frigerio, H Bonadeo†, M Weissmann† and N V Cohan
Departamento de Física, Comisión Nacional de Energía Atómica, Avenue del Libertador 8250, (1429) Buenos Aires, Argentina

Received 3 November 1982, in final form 14 February 1983

Abstract. The vibrational density of states of disordered $Xe_{1-x}Cs_x$ and $Xe_{1-x}Kr_x$ crystals is studied for $x \leqslant 0.05$. It is obtained as an average of local densities of states, which are calculated by the continued-fraction method. Two sets of asymptotic values for this expansion are used for a satisfactory approximation of both the main band and the minority peaks outside it. The use of a bond-stretching coordinate basis allows a physical interpretation of each local density of states and also gives simple kinetic and force constant matrices. The drawback of overcompleteness of this basis is easily overcome.

1. Introduction

In this paper we study theoretically the vibrational properties of disordered FCC mixed systems of the type $A_{1-x}B_x$, where A is a rare gas. Calculations for these systems have been performed only for very low (less than 1%) impurity concentrations (Hartmann and Elliott 1967, Martin 1967, Cohen and Klein 1974). This implies that the probability of finding two or more neighbouring impurity atoms is extremely low and therefore the systems consist of isolated impurities embedded in the host lattice. Even for this case calculations are rather involved and several approaches of the mean-field and other types have been proposed (Myles and Dow 1979, Herscovici and Fibich 1980). The main effect of the impurities is to activate optically the vibrational modes of the pure crystal. This effect has been observed experimentally (Keeler and Batchelder 1972) but at such low concentrations that the impurity modes are too weak to be observed. On the other hand, the electronic spectra of these systems (when B is a metal atom) have received a great deal of attention (Meyer 1978) and the peaks corresponding to clusters of several impurities have been observed. The rare-gas–metal binary materials are also interesting because they illustrate the well known insulator–metal transition (Swenumson *et al* 1981).

In this work we calculate the vibrational density of states of the rare-gas crystal doped with another rare gas or with an alkali metal, for concentrations up to 5% which implies taking into account a non-negligible probability of interaction between impurities. We have used a local-density-of-states formalism in conjunction with the continued-fraction algorithm. A method has been devised for a satisfactory description of both the majority

† Carrera del Investigador Científico, Conicet.

© 1983 The Institute of Physics

band region and the impurities modes, when these are outside it. We have chosen for our calculations Xe as the host lattice and Kr and Cs as the substitutional impurities. For these systems there exist reasonable data for the force constants and interatomic potentials. These data suggest that we may expect only slight relaxations of the lattice around the impurities. These distortions would introduce additional complications in the calculations and will be neglected here.

The examples chosen cover two interesting situations: for $Xe_{1-x}Cs_x$ the one-impurity mode gives resonances within the majority band and two-impurity modes are well outside it, while for $Xe_{1-x}Kr_x$ both modes lie close to the majority band edge. These two very different physical situations are a good test for the proposed method of calculation.

The results of this work are also meant to generate interest in the experimental measurements of these systems by optical and neutron scattering spectroscopy which in turn will allow us to improve the existing knowledge on the interatomic interactions of these mixed crystals.

2. Method

It is well known that the vibrational properties of rare-gas crystals are adequately represented by nearest-neighbour central forces of the van der Waals type. Therefore the interatomic bond stretchings become a natural choice of coordinate basis, allowing for a straightforward interpretation of local densities of vibrational states associated with particular bonds.

This basis also has the advantage of giving a diagonal force constant matrix $\mathbf{F}$ and an extremely simple kinetic energy matrix $\mathbf{G}$: in particular for FCC lattices only four different off-diagonal elements appear. However, the bond-stretching coordinate basis is overcomplete and contains a large number of redundancies which are associated with spurious zero-frequency modes. The symmetric form $\mathbf{F}^{1/2}\mathbf{G}\mathbf{F}^{1/2}$, is used for the dynamic matrix.

For the calculation of the vibrational density of states $n(\omega^2)$ of disordered systems of the $A_{1-x}B_x$ type with $x \ll 1$, and due to the lack of translational symmetry, it is usual to apply some kind of Green function formalism. In this work we approximate $n(\omega^2)$ by an average of local densities of states $n_i(\omega^2)$ where each $n_i(\omega^2)$ is calculated by the continued-fraction method (Haydock *et al* 1972) as

$$n_i(\omega^2) = -\frac{1}{\pi}\lim_{\varepsilon\to 0} \operatorname{Im} G_i(\omega^2 + i\varepsilon) \tag{1}$$

with

$$\begin{aligned} G_i(\omega^2) &= \left(\omega^2 - a_1^i - b_1^i g_1^i(\omega^2)\right)^{-1} \\ g_1^i(\omega^2) &= \left(\omega^2 - a_2^i - b_2^i g_2^i(\omega^2)\right)^{-1} \\ &\vdots \\ g_{n-1}^i(\omega^2) &= \left(\omega^2 - a_n^i - b_n^i g_n(\omega^2)\right)^{-1} \end{aligned} \tag{2}$$

and, in the limit,

$$g_n(\omega^2) = \left(\omega^2 - a(\omega^2)_\infty - b(\omega^2)_\infty g_n(\omega^2)\right)^{-1}. \tag{3}$$

To calculate the average we divide the crystal into two regions (Cohan and Weissmann 1977): a disordered cluster made up of the bond where the local density of states is calculated, which will be called the central bond, and its nearest-neighbour bonds giving a total of N_d atoms, and an ordered region surrounding the above cluster made up of N_0 majority atoms. We call $N_a = N_d + N_0$ the total number of atoms and N_b the total number of bonds. In both regions we keep the crystal structure of the pure A system unaltered thus not allowing for relaxation around the impurity atoms. The value of N_b is chosen to be large enough so that the last values a_n^i and b_n^i in equations (2) are calculated including all possible paths in a first-neighbour-type calculation. Finally, two choices for $a(\omega^2)_\infty$ and $b(\omega^2)_\infty$ are made, according to the frequency zone in which we are interested. For frequencies $\omega \leqslant \omega_{\max}^{A}$, the band limit frequency for the pure A crystal, we choose $a(\omega^2)_\infty = a_\infty^A$ and $b(\omega^2)_\infty = b_\infty^A$ where a_∞^A and b_∞^A correspond to the pure A crystal so that all the $n_i(\omega^2)$ are obtained from equation (1) only if $\omega \leqslant \omega_{\max}^{A}$. Thus, for each configuration i we obtain by this procedure the shape of the local density of states within the main band. To obtain the peaks outside the A band, if they exist, we first determine their positions approximately from the poles of the real part of the Green function with $n = 1$ and a_∞^A and b_∞^A in equation (3). Then we use an *ad hoc* pair of values $a(\omega^2)_\infty = a_\infty^*$ and $b(\omega^2)_\infty = b_\infty^*$ for all the configurations to allow these peaks also to be obtained from equation (1): that is we use here an 'enlarged' energy (frequency) band. Thus for each configuration i, the local density of states $n_i(\omega^2)$ is always calculated with equations (1), (2) and (3) and with

$$\left.\begin{aligned} a(\omega^2)_\infty &= a_\infty^A \\ b(\omega^2)_\infty &= b_\infty^A \end{aligned}\right\} \qquad \text{for } \omega \leqslant \omega_{\max}^{A}$$

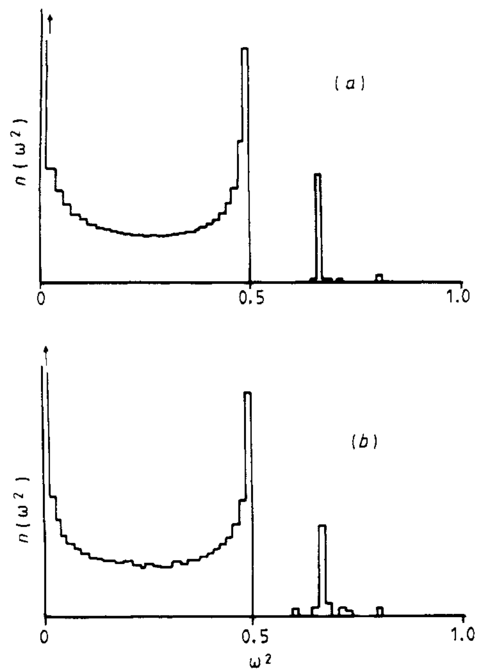

Figure 1. Vibrational density of states for the one-dimensional mass disordered chain. Impurity-to-host mass ratio 1:2; concentration $x = 0.05$. (*a*), present work; (*b*), exact calculation (Dean 1972).

and

$$\left.\begin{aligned} a(\omega^2)_\infty &= a^*_\infty \\ b(\omega^2)_\infty &= b^*_\infty \end{aligned}\right\} \qquad \text{for } \omega > \omega^{\mathrm{A}}_{\max}.$$

We tested this procedure for a one-dimensional isotopically disordered system and compared it with the numerical results of Dean (1972). From figure 1 we see that the results from the present calculation (shown in this case as a histogram), which only averages configurations within first neighbours and which does not use a self-consistent form for the environment field, agree very well in the shape of the main band and in the heights of the peaks with those of the direct method. The use of two different sets of values for $a(\omega^2)_\infty$ and $b(\omega^2)_\infty$ avoids spurious deformations in the majority band which occur only if the 'enlarged' energy band is used throughout, as in previous work (Cohan and Weissmann 1977).

The zero-frequency δ-peaks due to the redundant coordinates are broadened by the use of the continued-fraction approximation which is cut off at level n. The integrated intensity of these resulting peaks varies from case to case due to the different projections of the zero-frequency modes upon the corresponding local density of states. The level n has to be chosen so that these peaks become narrow enough to remain fairly isolated, thus not interfering with the genuine band structure. They are then easily subtracted for each local density of states $n_i(\omega^2)$.

3. The FCC disordered configurations

For an FCC lattice the total number of configurations 2^{N_d} is extremely large since each bond has 22 neighbouring bonds and thus the number of atoms in the disordered cluster is $N_\mathrm{d} = 20$ (four atoms are shared by eight bonds). Each bond has four different types of first-neighbour bond, making angles of 60, 90, 120 and 180 °. There are eight bonds of the first type, four of the second, eight of the third and two of the last type.

$$P_r = \sum_{s=1}^{r} \binom{N_\mathrm{d}}{s} x^s (1-x)^{N_\mathrm{d}-s}$$

is a measure of the contributions of the configurations, with up to r impurities, to the

Table 1. Values of

$$P_r = \sum_{s=1}^{r} \binom{N_\mathrm{d}}{s} x^s (1-x)^{N_\mathrm{d}-s}$$

for the FCC lattice $A_{1-x}B_x$ where $N_\mathrm{d} = 20$, as a function of x and r, for low values of r and x.

r	$\binom{20}{r}$	x			
		0.01	0.05	0.1	0.2
1	20	0.983	0.736	0.392	0.069
2	190	0.999	0.925	0.677	0.206
3	1140	1.000	0.984	0.867	0.412
4	4845		0.997	0.957	0.630
5	15504			0.989	0.805
6	38760				0.914

total density of states. From table 1 we notice that the number of configurations that has to be taken into account grows enormously with x. In our calculations we will consider concentrations up to 5%, for which the inclusion of only one and two impurity configurations seems satisfactory.

We shall take into account the fact that the number of independent configurations is reduced by symmetry. As the 23-bond cluster has D_{2h} point symmetry each configuration can be repeated at most eight times (the number of symmetry operations of the D_{2h} group), although some higher-symmetry configurations appear only one, two or four times (the orders of the subgroups of D_{2h}). Using group theoretical considerations it can be shown that there are only five independent one-impurity configurations and 37 two-impurity ones. A disordered configuration i will be represented schematically by the central bond and the bonds (if any) which contain impurity atoms. In figure 2 we show some relevant one- and two-impurity configurations. The labelling in figure 2 will be used throughout.

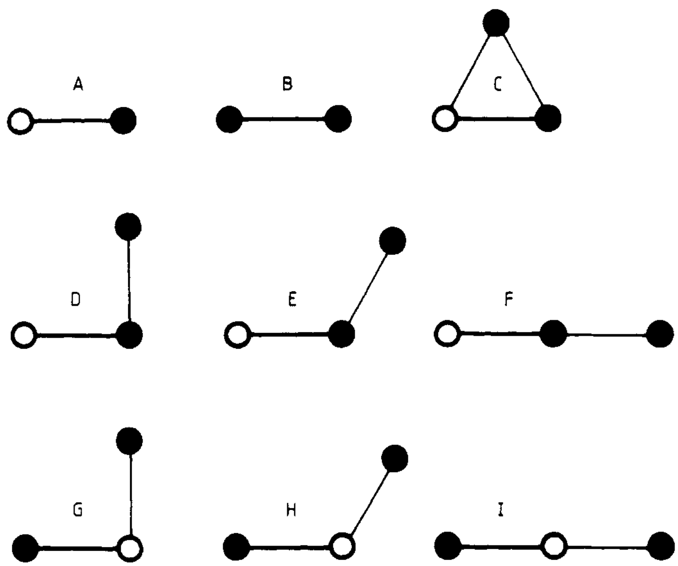

Figure 2. Relevant configurations. The open circles represent the majority atoms and the full circles the impurities. In all the configurations we show only the central bond (bold lines) and the bonds (if any) which contain impurity atoms.

4. The parameters for $Xe_{1-x}Cs_x$ and $Xe_{1-x}Kr_x$

In table 2 we show the interatomic force constants used in our calculations and some relevant interatomic distances. Lennard-Jones potentials provide an adequate description for the rare-gas interactions, and therefore the force constants for Xe–Xe and Kr–Kr were obtained from the corresponding Lennard-Jones parameters (Kittel 1967). The Xe–Kr force constant was taken from Schneider (1973). The force constants for the Xe–Cs and Cs–Cs interactions were taken from calculations for the dimers by Baylis

Table 2. Equilibrium distances r_e, inverse masses μ and force constants k for $Xe_{1-x}Cs_x$ and $Xe_{1-x}Kr_x$ mixed crystals. All values are given in units of the Xe crystal data: $r_e = 4.46$ Å, $\mu_{Xe} = (131.3\ \text{au})^{-1}$ and $k_{Xe\text{-}Xe} = 1.154 \times 10^3\ \text{erg cm}^{-2}$.

	r_e	μ	k
Xe–Cs	1.22	0.994	0.3(0.7)
Cs–Cs	1.04	0.988	5.97
Xe–Kr	0.90	1.284	1.20
Kr–Kr	0.92	1.567	0.84

(1969) and Ogilivie (1981) respectively. From the interatomic distances shown in table 2 we notice that the materials selected are such that we expect only slight distortions of the majority lattice, neglected in these calculations, due to the presence of impurities. Obviously, any distortion of the lattice around isolated impurities and cluster impurities implies changes in the host force constants as well as in the Xe–impurity and impurity–impurity force constants, which can be evaluated properly if a relaxed crystal is considered. We did not relax the crystal and used all the force constants calculated at the corresponding dimer interatomic distances which seems to us an adequate first approximation to the problem. The use of modified host–impurity and impurity–impurity force constants calculated at the host equilibrium distance imply modifications of the force constants which are too large, as has already been observed by Cohen and Klein (1974). However, in the particular case of Xe–Cs where the interatomic dimer distance is considerably larger than the Xe crystal lattice constant we have considered the possibility that the resulting compression may cause an increase in the corresponding force constant and therefore we also performed calculations with a higher value.

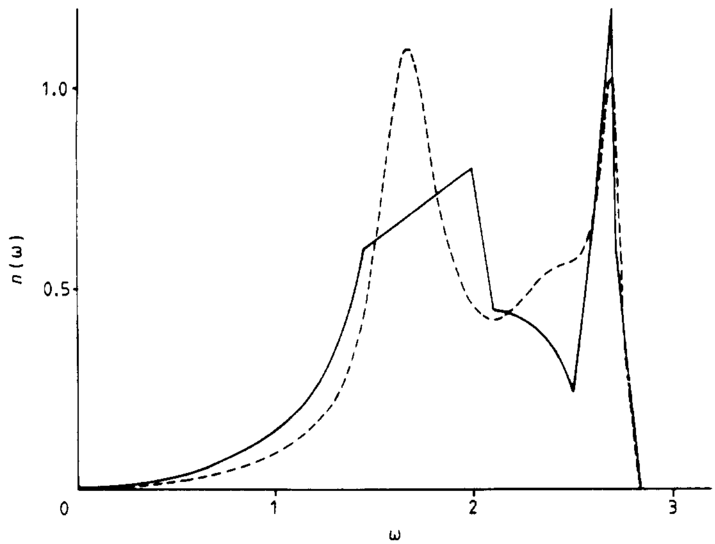

Figure 3. Density of states for the FCC crystal with nearest-neighbour central forces. Broken curve, this work; full curve, exact calculation (Rehr and Alben 1977).

5. Results and discussion

5.1. Pure Xe crystal

The densities of states of a number of quite different FCC monoatomic lattices (e.g. Cu and Ar (Rehr and Alben 1977)) are extremely similar and can be well represented by nearest-neighbour central forces. Much more elaborate force fields produce only slight alterations in the shape of $n(\omega)$, and thus we consider, as mentioned before, in all that follows only central-force nearest-neighbour interactions. In figure 3 we show the results of two calculations for the monoatomic FCC lattice: an exact Born–von-Karman calculation and a calculation with the method outlined in § 2 with $n = 4$ in equation (3). The agreement between the two curves is satisfactory taking into account that the continued fraction has been cut off at a very low order. However, this order already implies a total number of atoms $N_a = 652$ and of bonds $N_b = 3311$. Increasing slightly the order n implies increasing the number of bonds enormously. With this value of $n = 4$ the maximum due to the redundancies centred at zero frequency is already well isolated. Thus, the value of $n = 4$ seems to be an adequate compromise between reasonable accuracy and limited computing time.

5.2. The $Xe_{1-x}Cs_x$ crystal

The masses of the Xe and Cs atoms are extremely close and therefore the system exhibits essentially force constant disorder. As the Xe–Cs force constant, $k_{\text{Xe-Cs}}$, is smaller than $k_{\text{Xe-Xe}}$ while $k_{\text{Cs-Cs}}$ is larger (table 2), we expect that the one-impurity configuration will

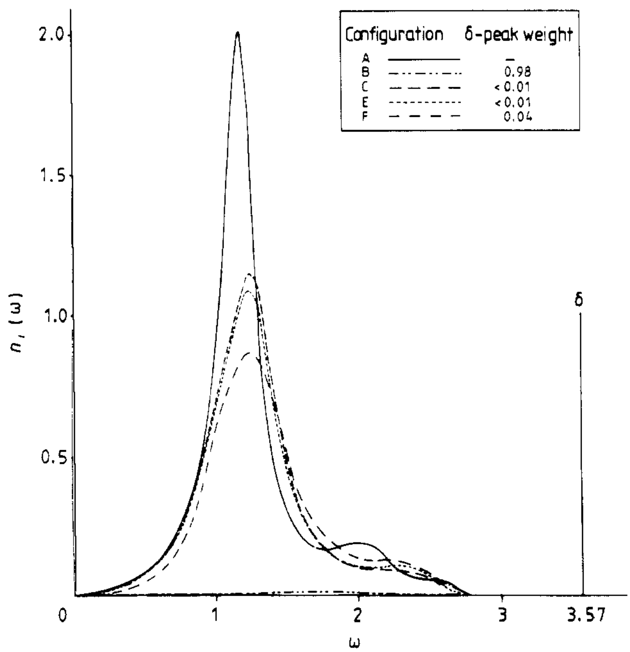

Figure 4. Local densities of states for XeCs, $k_{\text{Xe-Cs}} = 0.3$.

give rise to resonances within the main band, and the nearest-neighbour two-impurity configurations will give rise to peaks outside the main band. In figure 4 we show local densities of states for some relevant configurations. Of the five one-impurity configurations, only configuration A of figure 2 gives the expected resonance. The other ones, which have the impurity atom outside the central bond, have $n_i(\omega)$ very similar to that of pure Xe. The resonance modes are coupled to some crystal modes associated with the lower-frequency majority band which, in the local projection, appear as shoulders. The position of the resonance is shifted towards higher frequencies when a larger k_{Xe-Cs} is used (figure 5); the shift, however, is smaller than that expected from a simple force constant ratio picture due to the above-mentioned coupling.

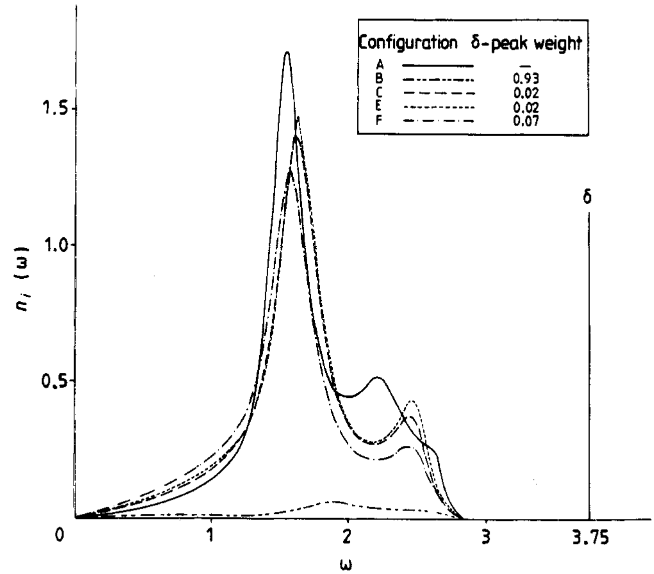

Figure 5. Local densities of states for XeCs, $k_{Xe-Cs} = 0.7$.

There are several groups of two-impurity configurations. Configuration B of figure 2 almost gives a δ-peak well outside the majority band and a very small contribution within it (see figures 4 and 5). It is interesting to note that the position of this two-impurity peak depends not only on k_{Cs-Cs} but also on k_{Xe-Cs}. This is so because although the Cs_2 stretching vibration is practically uncoupled with the rest of the crystal normal modes, the Cs_2 cluster vibrates against the framework of the Xe atoms and thus the k_{Cs-Xe} is involved in the motion. Configurations C, D, E and F all have two neighbouring impurities, one of which is in the central bond. Their main contribution consists of the one-impurity resonance peak. The two-impurity peak appears very weakly except in configuration D, in which the bond angle is 90°, and it does not show up (see inset of figure 4). Configurations G, H and F are essentially of the one-impurity type. All other configurations show very slight deviations from the pure Xe crystal density of states.

In figure 6 we show the total density of states $n(\omega)$ for $x = 0.01$ and 0.05 for $k_{Xe-Cs} = 0.3$. Minor changes in the majority band are observed with respect to pure Xe. The one-impurity peak shows at $\omega \simeq 1.2$ for the 5% concentration and the two-impurity quasi-δ-peak appears with a weight of the order of x^2. For $k_{Xe-Cs} = 0.7$ (figure 7) the

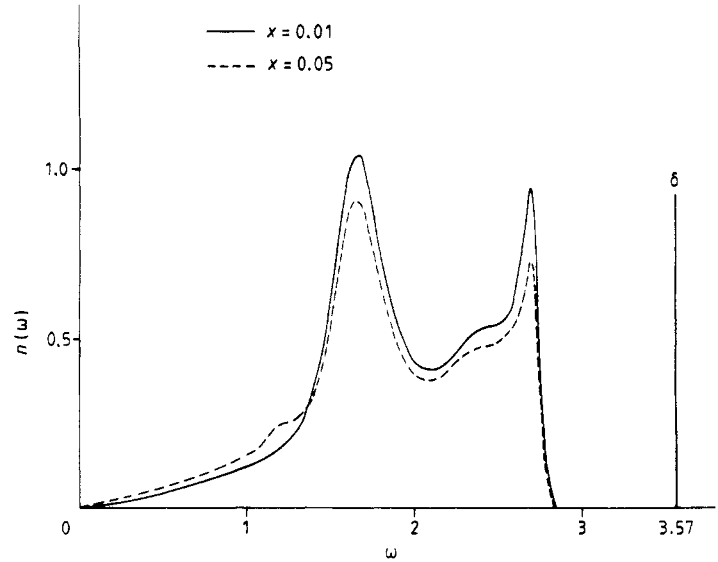

Figure 6. Density of states for $Xe_{1-x}Cs_x$, $k_{Xe\text{-}Cs} = 0.3$.

one-impurity peak is masked by the low-frequency majority band peak and the two-impurity peak is shifted towards higher frequencies, as noted before. Furthermore, the high-frequency majority band peak is perturbed slightly for the $x = 0.05$ concentration.

5.3. *The* $Xe_{1-x}Kr_x$ *crystal*

In contrast with the previous case the mass of the impurity is considerably lower than that of Xe and therefore we will have mass and force constant disorders. From the

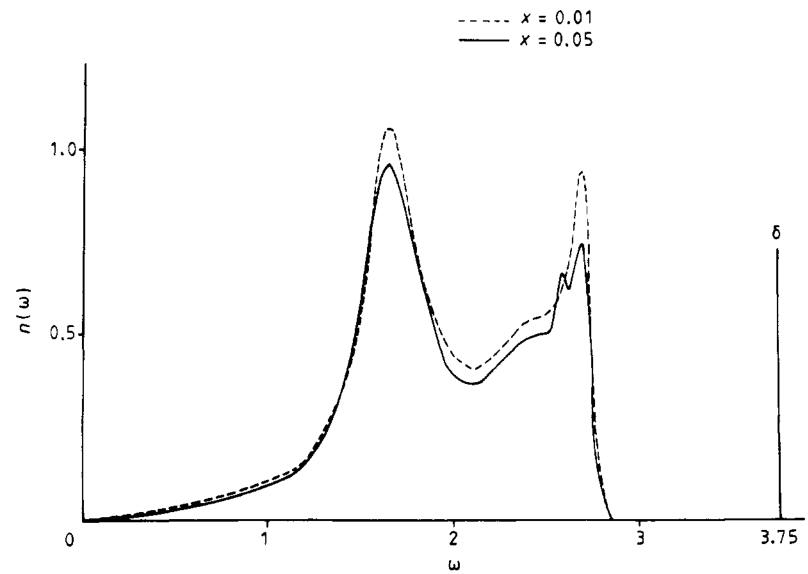

Figure 7. Density of states for $Xe_{1-x}Cs_x$, $k_{Xe\text{-}Cs} = 0.7$.

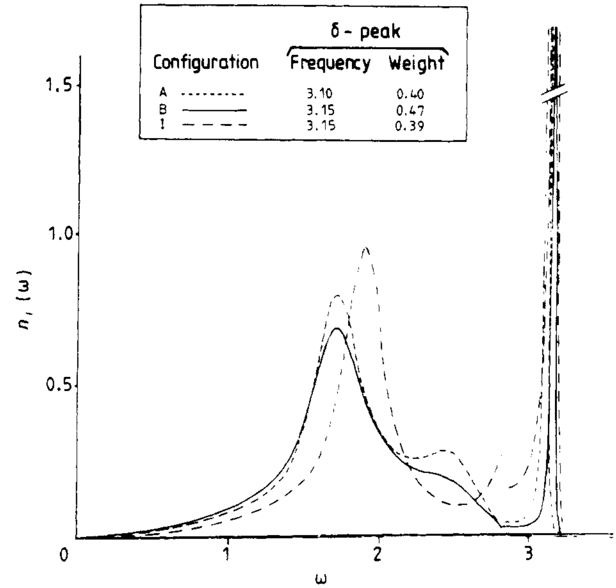

Figure 8. Local densities of states for XeKr (configurations A, B and I).

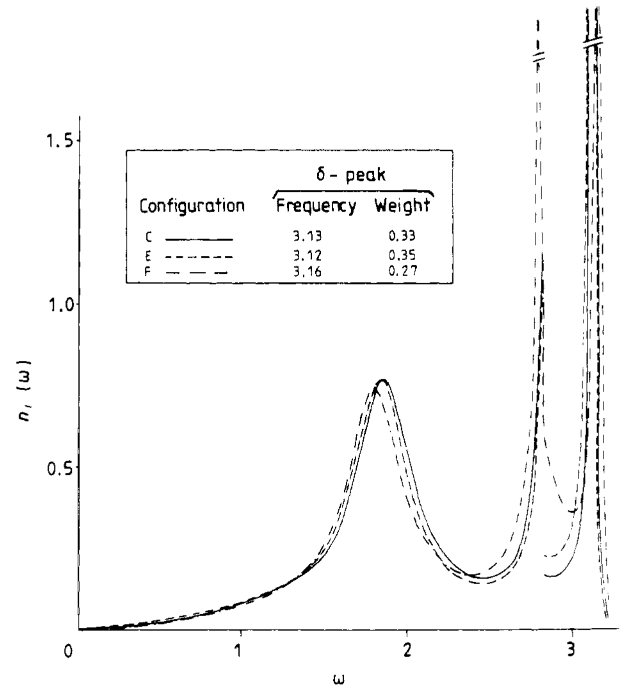

Figure 9. Local densities of states for XeKr (configurations C, E and F).

mass-to-force-constant ratios (table 2) it is expected that both one- and two-impurity peaks will be outside the majority band.

Figures 8 and 9 show the local densities of states $n_i(\omega)$ for some relevant configurations. All of them present a narrow peak outside, but near, the majority band limit. The one-impurity configuration A has its narrow peaks at $\omega = 3.10$ while the two-impurity configuration B contributes at $\omega \simeq 3.15$. These frequencies are very close and each of the remaining configurations shows a peak at a nearby frequency. In the configurations of figure 8 the low-frequency host-lattice band remains, although somewhat shifted, while the high-frequency band has disappeared.

We recall that $n_i(\omega)$ for $\omega \leqslant 2\sqrt{2}$ (the majority band limit) is calculated with $a(\omega^2)_\infty = a_\infty^{\mathrm{A}}$ and $b(\omega^2)_\infty = b_\infty^{\mathrm{A}}$ while for $\omega > 2\sqrt{2}$ the 'enlarged' energy band values are used. Therefore at $\omega = 2\sqrt{2}$ there may be, in principle, a discontinuity. For configurations A and B where $n_i(\omega)$ around $\omega = 2\sqrt{2}$ is small the matching is excellent. For configuration I the cutting of the band while $n_i(\omega)$ is still considerable produces a spurious rise.

Configurations C, E and F in figure 9 show a peculiar behaviour in that they present a very sharp peak inside the majority band but almost at its limit. These peaks are not spurious as they are revealed by the calculations with both sets of a_∞ and b_∞. They correspond to the high-frequency host lattice band which has been shifted and they are probably calculated to be too narrow because they lie at about $\omega \approx 2\sqrt{2}$. In all cases (see insets of figures 8 and 9) due to the proximity of the one- and two-impurity peaks to the band limit the local projection of the pure-crystal modes is considerable, in contrast with $Xe_{1-x}Cs_x$ crystal, where each local density of states contributes either inside or outside the majority band. All the other configurations are essentially similar to pure Xe except for the fact that the peaks are shifted slightly towards each other.

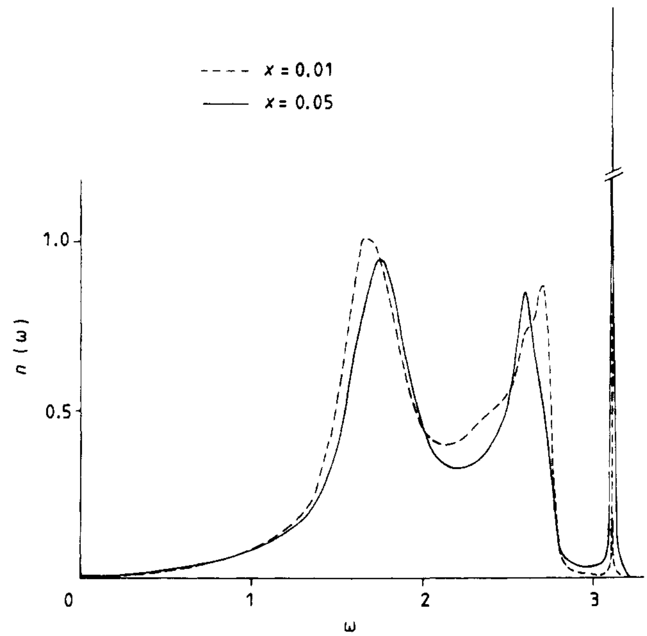

Figure 10. Density of states for $Xe_{1-x}Kr_x$.

In figure 10 we show the total density of states $n(\omega)$ for $x = 0.01$ and 0.05. The peaks inside the majority band shift towards each other with increasing concentration, an effect which could, in principle, be observed experimentally, The density of states between the band edge and the peak due to the impurities is non-negligible and the peak itself has a finite band width. The total area outside the majority band is about 5‰ for $x = 0.01$ and 2% for $x = 0.05$.

It should be noticed that if the Xe–Kr and Kr–Kr interatomic distances in the Xe host lattice were larger than their dimer values of 0.90 and 0.92 (table 2) the corresponding force constants would decrease and the impurity peak outside the majority band could disappear.

Although we have not performed calculations for Kr doped with Xe (Xe_xKr_{1-x}, $x \ll 1$) from the force constants and mass data of table 2, we expect the one-impurity Xe peak to lie slightly outside the majority band, around $\omega \approx 3$ or even lower, in agreement with the conclusions of Cohen and Klein (1974) who obtain this peak at $\omega = 2.88$ (52 cm^{-1}) or, at most, at $\omega = 3.05$ (55 cm^{-1}).

6. Conclusions

The method of calculation presented in this work has proved to be a satisfactory approach to the study of the vibrational density of states of mixed crystals. It provides a reasonable description of both the features of the majority band and the impurity peaks which fall outside it.

As stated in § 2, in a central-force problem, the natural choice for the basis of the calculations is that of bond stretchings since the potential energy depends only on the relative nearest-neighbour distances. When, as in the present work, one considers a cluster made up of a bond and all bonds attached to its end atoms, one is selecting some pairs of second, third and fourth neighbour atoms. These further neighbour atoms are precisely those which will be more relevant to the vibrations of the bond.

One practical disadvantage of this basis is that it produces redundancies which enlarge the dynamic matrix artificially. However, this drawback is compensated by the fact that the number of non-zero matrix elements in each row is less than for a cartesian atomic basis. In our case the number of redundancies is roughly half the total number of bonds N_b and there are 23 non-zero elements in each row, while in the atomic basis the 13 nearest-neighbour atoms produce 39 non-zero elements.

Some interesting conclusions can be derived from the observation of the local densities of states in this bond-stretching basis. Although we have calculated $n_i(\omega)$ for the 5 one-impurity and the 37 two-impurity configurations many of them look very much alike, and this fact enables us to group them into a few categories. For instance for $Xe_{1-x}Cs_x$ we have only four groups: (i) configuration A, (ii) configuration B, (iii) configurations C to I, (iv) all the rest. This grouping may be of great aid when calculations for higher concentrations are performed. For example, for $x = 0.1$ we certainly need to include three-impurity and possibly four-impurity configurations (see table 1). There are already 169 distinct three-impurity configurations and their inclusion makes the calculations considerably lengthy. The above-mentioned grouping suggests that it may be possible to assimilate many of the configurations of three and more impurities to specific configurations of less impurities thus reducing significantly the number of truly new configurations to be computed.

Acknowledgments

This work was partially supported by CONICET Grant No 8382c/81.

We are grateful to the referees for bringing to our attention the paper of Cohen and Klein.

References

Baylis W E 1969 *J. Chem. Phys.* **51** 2665
Cohan N V and Weissmann M 1977 *J. Phys. C: Solid State Phys.* **10** 383
Cohen S S and Klein M L 1974 *J. Chem. Phys.* **61** 3210
Dean P 1972 *Rev. Mod. Phys.* **44** 127
Hartmann W M and Elliott R J 1967 *Proc. Phys. Soc.* **91** 187
Haydock R, Heine V and Kelly M J 1972 *J. Phys. C: Solid State Phys.* **5** 2845
Herscovici C and Fibich M 1980 *J. Phys. C: Solid State Phys.* **13** 4463
Keeler G J and Batchelder D N 1972 *J. Phys. C: Solid State Phys.* **5** 3264
Kittel C 1967 *Introduction to Solid State Physics* (New York: John Wiley) p 81
Martin T P 1967 *Phys. Rev.* **160** 686
Meyer B 1978 *Ber. Bunsenges. Phys. Chem.* **82** 24
Myles C W and Dow J D 1979 *Phys. Rev.* B **19** 4939
Ogilivie J F 1981 *Proc. R. Soc.* A **378** 287
Rehr J J and Alben R 1977 *Phys. Rev.* B **16** 2400
Schneider B 1973 *J. Chem. Phys.* **58** 4447
Swenumson R D, Leutwyler S and Even U 1981 *Phys. Rev.* B **24** 5728